frontiers in Energy Research

ORIGINAL RESEARCH
published: 14 May 2021
doi: 10.3389/fenrg.2021.670904

Synthesis of Bio-Cellulose Acetate Membrane From Coconut Juice Residues for Carbon Dioxide Removal From Biogas in Membrane Unit

Attaso Khamwichit[1,2], *Sakkarin Wattanasit*[1] *and Wipawee Dechapanya*[1,2]*

[1] *Department of Chemical Engineering, Walailak University, Nakhon Si Thammarat, Thailand,* [2] *Biomass and Oil Palm Research Center of Excellence, Walailak University, Nakhon Si Thammarat, Thailand*

The rapid growth of energy demand and consumption from fossil fuels has been of great concern since the last decade. Renewable energy, including biogas production from wastes, has been studied to ease up the energy crisis problems. This study aims to synthesize bio-cellulose acetate (CA) membranes from agricultural waste and to study its efficiency in the removal of CO_2 from biogas. The bio-CA membranes were synthesized from acetylation of bacterial cellulose (BC) and obtained from coconut juice residues (CJRs). The results showed that both chemical and physical characteristics of the bio-CA membrane were compared with those of the chemical CA membranes. The CO_2 removal capacity of the bio-CA membranes was tested in a membrane separation unit. The maximum CO_2 selectivity of 29.53 was achieved when using the bio-CA membrane with a thickness of 0.05 mm under the feed pressure of 0.1 MPa. Thick CA membranes exhibited better CO_2 selectivity performance, particularly at low operating pressure. However, the CO_2/CH_4 separation factor decreased in the high-pressure region, probably because of the plasticization of the gas components. Eco-efficiency was evaluated to determine the optimal process conditions. In terms of eco-efficiency, the results suggested that the optimal condition was a bio-CA membrane of 0.05-mm thickness and pressure of 0.1 MPa. The implication of this study is promoting a zero-waste environment in which the agricultural residues could be potentially used in the synthesis of high-value CA membranes for biogas purification applications in energy production.

Keywords: cellulose acetate membrane, biopolymer, CO_2 removal, biogas separation, agricultural waste utilization

OPEN ACCESS

Edited by:
Nidia S. Caetano, Instituto Superior de Engenharia Do Porto (ISEP), Portugal

Reviewed by:
Obulisamy Parthiba Karthikeyan, University of Houston, United States
Asim Laeeq Khan, COMSATS University Islamabad, Lahore Campus, Pakistan

***Correspondence:**
Wipawee Dechapanya
khamwipawee@gmail.com;
kwipawee@wu.ac.th

Specialty section:
This article was submitted to Bioenergy and Biofuels, a section of the journal Frontiers in Energy Research

Received: *22 February 2021*
Accepted: *14 April 2021*
Published: *14 May 2021*

Citation:
Khamwichit A, Wattanasit S and Dechapanya W (2021) Synthesis of Bio-Cellulose Acetate Membrane From Coconut Juice Residues for Carbon Dioxide Removal From Biogas in Membrane Unit. Front. Energy Res. 9:670904. doi: 10.3389/fenrg.2021.670904

INTRODUCTION

Biogas has become a promising source of renewable energy in recent times, particularly in developing countries where plentiful amounts of agricultural-related raw materials can be utilized in biogas production. Typically, biogas can be generated from an anaerobic fermentation process of various feedstocks containing organic materials. Generally, the composition of biogas is CH_4, CO_2, and other gaseous compounds, such as H_2S, N_2, and humidity (Adebayo et al., 2015).

However, biogas is usually pre-purified to remove impurities before use since those undesired components could potentially cause some inferior properties or damages in application processes. For example, CO_2, which is present in a relatively large quantity in biogas, can lower the heat value of used biogas, which results in high transportation costs. For the removal of CO_2 from biogas applications, membrane gas separation has become one of the emerging technologies over the traditional processes, such as pressure swing adsorption or cryogenic distillation (Moghadassi et al., 2014). The separation is mostly based on the sorption-diffusion mechanism of the gas components transporting through the dense membranes, in which there is a compromise between selectivity and permeability. A wide range of polymeric materials have reportedly been utilized and fabricated into membranes, such as polycarbonate (PC), polysulfone (PSF), polyimide (PI), ethyl acetate (EA), polyphenylene oxide, polydimethylsiloxane, and cellulose acetate (CA), suitable for CO_2 removal applications (Cerveira et al., 2018). Unlike other polymers, the CA membrane can be alternatively prepared *via* bioprocesses that involve fewer uses of hazardous monomers and solvents in the preparation stage. Bio-CA can be synthesized from low-price bacterial cellulose (BC) obtained from the cultivation of various indirect carbon sources, including wastewater from agricultural industries and fruit juices (Phruksaphithak et al., 2019). Since there are plenty of inexpensive food source alternatives for the uncomplicated preparation of BC, therefore, these bio-CA materials could be economically attractive due to their low-cost production. The fabrication of the material into suitable forms of product that have well-suited properties for the implemented applications remains a challenge. Many studies reported the use of CA membranes in various forms for CO_2 removal from various mixed gas systems, mostly in flat-sheet and spun hollow-fiber configurations (Chen et al., 2015; Sanaeepur et al., 2019). In general, pristine CA membranes exhibit inferior CO_2 separation from the mixed gas. Therefore, modifications of the membranes were commonly incorporated to increase the separation efficiency. For example, a study by Pak et al. (2016) reported the use of the hollow fiber CA membrane for CO_2/CH_4 separation. A relatively high CO_2 selectivity was achieved while maintaining a moderate permeability. Some additives, such as metal-organic frameworks (MOFs), which are capable of controlling the molecular sieving properties in gas separations, can be added to the membrane to improve the interaction between the membrane and the gas pairs that lead to superior separation performance. For instance, a study by Mubashir et al. (2020) found that NH_2_MIL-53(Al) was successfully incorporated into the CA/polydimethylsiloxane-based hollow fiber membrane to increase the CO_2/CH_4 separation factor of the binary gas mixture. Also, reinforcement would increase the strength of the membrane so that the membrane could withstand high operating pressure. A study by Moghadassi et al. (2014) reported that multi-walled carbon nanotubes (MWCNTs) were blended with CA to form a composite CA membrane that could tolerate high feed, resulting in an improved permeability of the gas product. Besides the hollow-fiber type, flat sheet membranes could also be a competitive alternative since they require a simpler and more economical fabrication process. Mubashir et al. (2018a) suggested that flat-sheet CA membranes could be achieved by the solvent-casting technique using the N-methyl-1-2 pyrrolidone (NMP) as the fabricating solvent. The CO_2 removal performance results of some of those related studies on various CA membrane systems are shown in **Table 3**.

As described earlier, conventional methods to prepare CA-based membranes involve the use of synthesized CA obtained from the chemical process, and the fabrication of the membrane itself would require the use of solvents and/or chemical additives. However, a bioprocess approach could be utilized to prepare the CA membrane. Khami et al. (2014) reported that the CA could be synthesized from a fermentation process of banana peels using *Acetobacter xylinum*. Many factors affect the properties of the obtained CA involved in the bioprocess using *A. xylinum*, including cultivating temperature, pH, cultivation duration, glucose quantity (% Brix), and also the type or source of the substrate (Khami et al., 2019). Several research studies have shown that both CA and bio-CA membranes are generally recognized as biodegradable materials (Rivard et al., 1992, Buchanan et al., 1993, Komarek et al., 1993, Gu et al., 1993, Gardner et al., 1994, Elfiana et al., 2018). The biodegradation rate of bio-CA made from nata de coco was 5–28% per day (Elfiana et al., 2018). Whereas, under the enrichment culture, the CA film was able to degrade, 67% weight loss, within 2–3 weeks (Buchanan et al., 1993).

Alternative carbon sources using fruit juices for the biosynthesis of BC propose high productivity and low cost (Phruksaphithak et al., 2019). Among them, coconut juice residues (CJR) are abundant, left from coconut postprocessing in Thailand, especially in the southern area. Hence, this study focuses on the biosynthesis and fabrication of bio-CA membranes from BC obtained from the cultivation process of CJR. The two-step process involves the preparation of the cultivated BC flat sheet and the following acetylation of the BC to obtain bio-CA membrane. The potential use of the synthesized membranes for CO_2 removal from biogas application using membrane separation was studied in a binary CO_2/CH_4 gas mixed system. The CO_2 removal capability of the membranes was measured in terms of the CO_2 selectivity of the gas permeates. Finally, the concept of eco-efficiency was adapted as a tool to analyze the economic potential and the environmental impact of the proposed membrane separation process using bio-CA membranes to remove the CO_2. This study would fulfill the gap of the utilization of bio-CA membrane in the gas separation process. Thus, the implication of this work could be beneficial to the growing development of biogas utilization in high-efficiency energy production.

MATERIALS AND METHODS

Materials

Coconut juice residues, discarded after processing coconut milk, were obtained from a community market located in Thasala, Nakhon Si Thammarat, Thailand. Analytical grade of ammonium sulfate [$(NH_4)_2SO_4$] with purity >99.99% was purchased from QRec (Thailand). Ethanol (99.8% purity) was supplied by Sigma Aldrich (Bangkok, Thailand). Granulated

sugar was acquired from Mitr Phol Sugar Corp., Ltd. (Bangkok, Thailand). The acetic acid aqueous solution (5%v) was acquired from Nakornvitee Marketing Co., Ltd. (Wang Muang District, Thailand). The mixed gas of CO2/CH4 (40/60%v) was purchased from Linde (Thailand) Public Company Limited (Samut Prakan, Thailand).

CA Membrane Preparation

Acetobacter xylinum strains obtained from the Thailand Institute of Scientific and Technological Research (TISTR), Bangkok, Thailand was used for the biosynthesis of BC. This strain is widely used as it has the best yield of BC (Kongruang, 2008). Bacterium culture on Agar plates was prepared by transferring liquid culture aseptically into Petri plates, containing NA Agar medium, and incubated at 30°C for 3 days. The 3-day-old bacteria cells were inoculated into 25 ml of starter medium of hydrosulphite of sodium (HS) (Pa'e et al., 2011). The number of viable cells in the inoculum was determined by the pour plate technique with HS medium (Kongruang, 2008; Pa'e et al., 2011). Colonies were counted after 5 days of incubation at 30°C. The substrate for biosynthesis of BC was conducted by filtrating 1,000 ml of CJR using a filtration glass set (Rocker Model VF7cat.167200-07, Taiwan). The filtrated CJR was sterilized in an autoclave at 121°C for 15 min, and then, it was cooled down to room temperature. The sterilized CJR was added into a beaker containing 1 g of ammonium sulfate, 28 g of nutrient agar, and 100 g of glucose. The substrate mixture was stirred with the hotplate stirrer at 30°C until homogenization was obtained. Then, 5 mL of acetic acid and 100 mL of 40% by volume ethanol were added (Khami et al., 2019).

Acetobacter xylinum with the amount of 1×10^5 cfu/ml was added to 25 ml of the prepared substrate in the incubation plate with a diameter of 8 ± 0.3 cm. In this study, three dosages of *A. xylinum* were varied, 1×10^5, 1×10^6, 1×10^7 cfu/ml, to examine its effect on bio-CA production. The production of BC was accomplished under static culture in an incubator (Binder model BD115, Germany) at 40°C for 7 days (Pa'e et al., 2011, Lestari et al., 2014). During the cultivation period, the gelation of BC was formed. The degree of gelation of BC increased with time as the substrate medium was consumed. Various degrees of thickness of the prepared membranes was achieved by varying the amount of the initially used substrate of 20, 30, and 40 ml. The bio-CA membrane was fabricated from the cultivated BC through semi-acetylation. The acetylation process depends on the accessibility of cellulose fibers and the susceptibility of individual cellulose crystallites (Barud et al., 2008). After 7 days of cultivation, BC pellicle on the substrate surface was collected and soaked in distilled water at ambient temperature for 3 days. Bacterial cell debris was removed by boiling BC with 40 ml of 2% NaOH for 3 h at 60°C. After that, 40 ml of 40% ethanol was added, and BC was further boiled for another 3 h at the same temperature. Then, BC was dehydrated in an oven at 60°C for 3 h before blending into a mixture of 40 ml of acetic acid, 50 ml of toluene, and 0.2 ml of 60% perchloric acid. To remove any impurities and remaining reagents, BC was soaked in 40 ml of 75% ethanol for 2 h. BC was rinsed off by distilled water several times until the stinky odor was vanished and finally dried in a hot air oven model M100-800 (Memmert GmbH + Co. KG, Bangkok, Thailand) at 60°C for 8 h (Khami et al., 2019). The thickness values were randomly measured using a micrometer from 10 points covering the surface area of the whole membrane. Then, the average thickness of the bio-CA membranes was estimated; the results were confirmed by the measurement from the cross-sectional area using scanning electron microscope (SEM) analysis.

Effecting factors of BC production include pH, carbon source, % Brix, *A. xylinum* dosage, and temperature (Phruksaphithak et al., 2019). As suggested by previous studies in our research unit (Khami et al., 2014, 2019), the conditions for the cultivation of BC selected in this study included the following: pH (4–5), Brix (5–15%), and *A. xylinum* dosage (1×10^5-1×10^7 cell/ml). The set of experiments was designed using Box–Behnken design (BBD) in the response surface methodology (RSM) (Tafreshi et al., 2017). Yields of BC in terms of the conversion of CJR into BC (BC to CJR solution weight ratio) were calculated from the results of those experiments. The results from BC yield were then put into a response optimizer to determine the optimum conditions for the biosynthesis of BC.

Characterization of CA Membrane

Morphology Properties

The microstructure of the CA membrane from CJR was examined using an SEM (Model Merlin Compact, Carl Zeiss Co., Ltd., Bangkok, Thailand). The CA membrane was dried in a hot air oven (model FD115; Franz Binder GmbH & Co., Bangkok, Thailand) at 65°C for 6 h. Then, it was taken off from the oven and put in a desiccator (model RT-48C; Eureka Design Co., Ltd., Pathum Thani, Thailand) until it cooled to ambient temperature. The dried CA membrane was mounted on carbon stubs, sputter-coated with gold, and examined in a Jx A-840 SEM (Jeol, USA). The images from the SEM were analyzed with Microsun 2000/s image analysis software to obtain data on the nanostructure of the CA membrane. The magnification of the image analysis was 10,000× at 5 kV.

Tensile Stress

The tensile stress of the synthesized CA membranes with three different degrees of thickness was tested using a tensile stress machine (model DSS-10T; Shimadzu, Japan). The testing procedure followed ASTM D638 standard. CA membrane samples, with various degrees of thickness (0.03, 0.04, and 0.05 mm) and a width of 40 mm, were placed in the clamps. The tensile force was increased until the sample was torn, in which six replications were examined.

Fourier Transform Infrared (FTIR) Spectra Analysis

Attenuated total multiple reflection (ATR) Fourier Transform IR (FTIR) spectrometer (model Tensor 27; Bruker, Germany) was used to analyze functional groups of the chemical structure of the CA membrane. The analysis procedure followed the ATR-FTIR technique. The spectrum used in the study was in a wavelength range of 400–4,000 cm^{-1}.

Thermo Gravimetric Analysis

Thermogravimetric analysis (TGA was conducted using Pyris1 TGA (Perkin Elmer, Ltd., Bangkok, Thailand). Change of the thermal property of dried CA membranes was estimated by

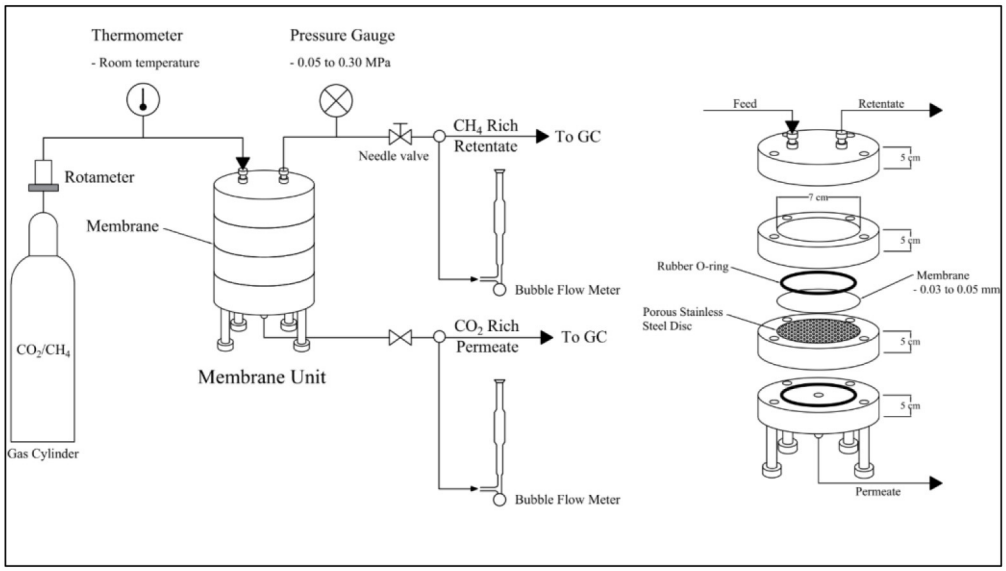

FIGURE 1 | Membrane separation unit.

differential scanning calorimetry (DSC) (model DSC6000; Perkin Elmer, Ltd., Bangkok, Thailand). The analysis proceeded as instructed by the ASTM E1131, ISO 11358 standard. The weight of the sample used in the analysis was 1 g, and its surface was 1 cm × 1 cm. The TGA temperature was heated from 25 to 700°C at 10°C/min, while DSC temperature was heated from 30 to 440°C at 10°C/min. Three replications for each test were performed.

Membrane Separation Unit

To study the gas permeation of CO_2 from the gas mixture using the synthesized CA membrane from CJR, the membrane separation unit, as displayed in **Figure 1**, was designed and constructed. The membrane separation unit was constructed from aluminum consisting of four layers. The plate at one end of the membrane unit was connected to the feed inlet and retentate outlet. The CA membrane was placed on a porous stainless-steel disc located between the feed and the permeate chamber. The permeate outlet was connected to the endplate of the permeate chamber side. Rubber O rings were used for gas leak prevention from each compartment.

From **Figure 1**, the gas mixture was fed to the top of the membrane separation unit through a regulator. The gas flow rate was measured and controlled using a rotameter. The separation of CO_2 from the gas mixture was studied using the gas mixture of 40/60% CO_2/CH_4 under the following conditions: a pressure range of 0.05–0.30 MPa, temperature of 30°C, CA membrane thickness of 0.03 ± 0.005, 0.04 ± 0.005, and 0.05 ± 0.005 mm.

Gas permeability and gas selectivity of pure gas was calculated using Equations (1) and (2) (Basu et al., 2010) while gas permeability and gas selectivity of mixed gas were calculated using Equations (3) and (4):

$$P = \frac{\boldsymbol{Q} * \boldsymbol{l}}{\boldsymbol{A}\Delta\boldsymbol{p}} = \frac{\boldsymbol{Q} * \boldsymbol{l}}{\boldsymbol{A}\left(\boldsymbol{p_{feed}} - \boldsymbol{p_{perm}}\right)} \tag{1}$$

where P : the gas permeability coefficient of component i
Q: feed flow rate (cm^3/s)
l : the selective layer thickness of the membrane
A: the area of the membrane
P: the pressure difference across the membrane
P_{perm}: permeate pressure
P_{feed}: feed pressure
The pure-gas selectivity ($\alpha_{a/b}$):

$$\alpha_{a/b} = P_a/P_b = \frac{Q_a\left(p_{feed,b} - p_{perm,b}\right)}{Q_b\left(p_{feed,a} - p_{perm,a}\right)} \tag{2}$$

where $\alpha_{a/b}$: the selectivity (a/b)
Mixed-gas permeability of each component:

$$P_i = \frac{Q * x_{perm,i} * l}{A\left(p_{feed}x_{feed,i} - p_{perm}x_{perm,i}\right)} \tag{3}$$

where P_i: the gas-mixed permeability coefficient of component i
$x_{perm,i}$: mole fraction of component i in the permeate stream
$x_{feed,i}$: mole fraction of component i in the feed stream
Mixed-gas selectivity

$$\alpha_{a/b} = \frac{\boldsymbol{x_{perm,a}}\left(\boldsymbol{p_{feed,b}} - \boldsymbol{p_{perm,b}}\right)}{\boldsymbol{x_{perm,b}}\left(\boldsymbol{p_{feed,a}} - \boldsymbol{p_{perm,a}}\right)} \tag{4}$$

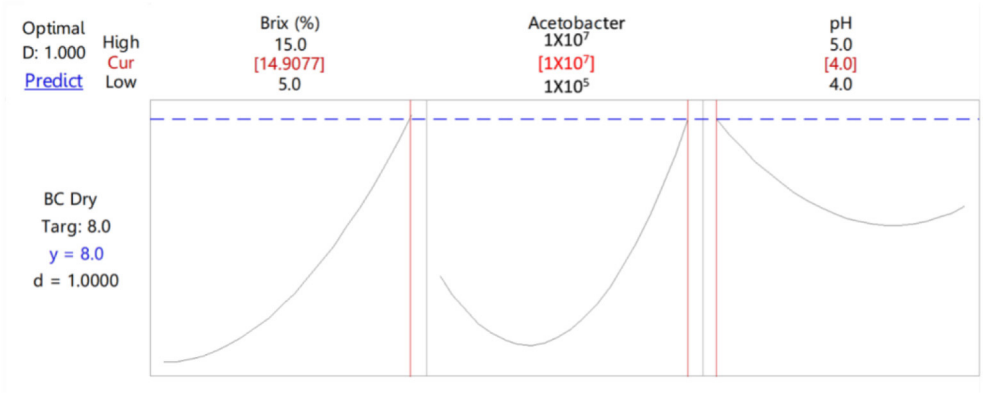

FIGURE 2 | Optimum conditions for bacterial cellulose (BC) cultivation from coconut juice residues (CJRs) by *Acetobacter xylinum*.

Eco-Efficiency

Eco-efficiency is an inclusive indicator for performance measurement of product, process, and service (PPS) system in terms of environmental impact and resource use and economic development (Liu et al., 2020). It is an effective tool for sustainable development that follows the ISO14045 standard (Environmental management: Eco-efficiency assessment of product systems) (Changwichan et al., 2018). In general, eco-efficiency was obtained from the ratio of product or service value to the environmental impact such as the consumption of energy, materials, and water or generated greenhouse gas emissions and carbon dioxide emissions. The concept equation of eco-efficiency can be calculated as Equation (5) (Heilala et al., 2014).

$$Eco-efficiency = \frac{Value\ of\ the\ product,\ process\ or\ service(PPS)}{Environmental\ impact\ of\ the\ PPS} \quad (5)$$

In this study, to apply the concept of sustainability and eco-efficiency indicators, the eco-efficiency Equation (6) was modified. The value of PPS was represented by CO_2 selectivity. The operating cost of the membrane unit was calculated from the cost of the gas mixture used in the performing experiment. The total operating cost of bio-CA membrane produced by *A. xylinum* including chemicals used and electricity was calculated using with following equation.

$$Eco-efficiency = \frac{E_d}{E_c} \quad (6)$$

where E_d: CO_2 selectivity

E_c: Cost of bio-CA membrane production and operating of the membrane unit.

RESULT AND DISCUSSION

Biosynthesis of BC From CJR and Its Optimum Conditions for the Cultivation

The optimum cultivation conditions were determined using the Surface optimizer. **Figure 2** illustrates that, within the ranges of studied parameters, the optimum conditions of BC production were 14.9% Brix, 1×10^7 cfu/ml of *A. xylinum*, and pH of 4. Thus, these conditions were controlled in the cultivation of BC from CJR. *A. xylinum* used CJR as the carbon source in the production of BC. The carbon source of CJR used in the study was 6,000–12,000 mg/l. The high-performance liquid chromatography (HPLC) analysis of the remaining substrate found the highest concentration of sucrose, glucose, fructose, lactic acid, and acetic acid at 4.99, 7,62, 14.04, 1.38, and 0.38 g/L, respectively. Throughout cultivation, pH gradually decreased with the production of lactic acid and acetic acid by *A. xylinum*. Therefore, pH that is suitable for BC cultivation should not be <4.

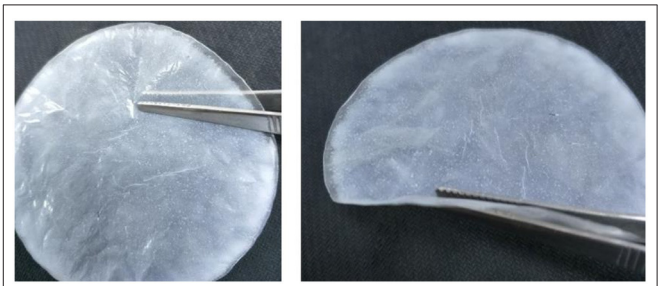

FIGURE 3 | Cellulose acetate (CA) membrane from CJRs.

The bio-CA membranes, as shown in **Figure 3**, were fabricated through the acetylation from BC with the thickness of 0.03 ± 0.005, 0.04 ± 0.005, and 0.05 ± 0.005 mm. Dry weights of the CA-0.03, CA-0.04, and CA-0.05 membranes were ~0.11, 0.28, and 0.42 g, respectively.

Morphological and Structural Analysis of CA Membrane

The bio-CA membranes were obtained from the cultivation process, described earlier. In general, the thin solid membranes were flat sheet-like with some degree of roughness on the surface,

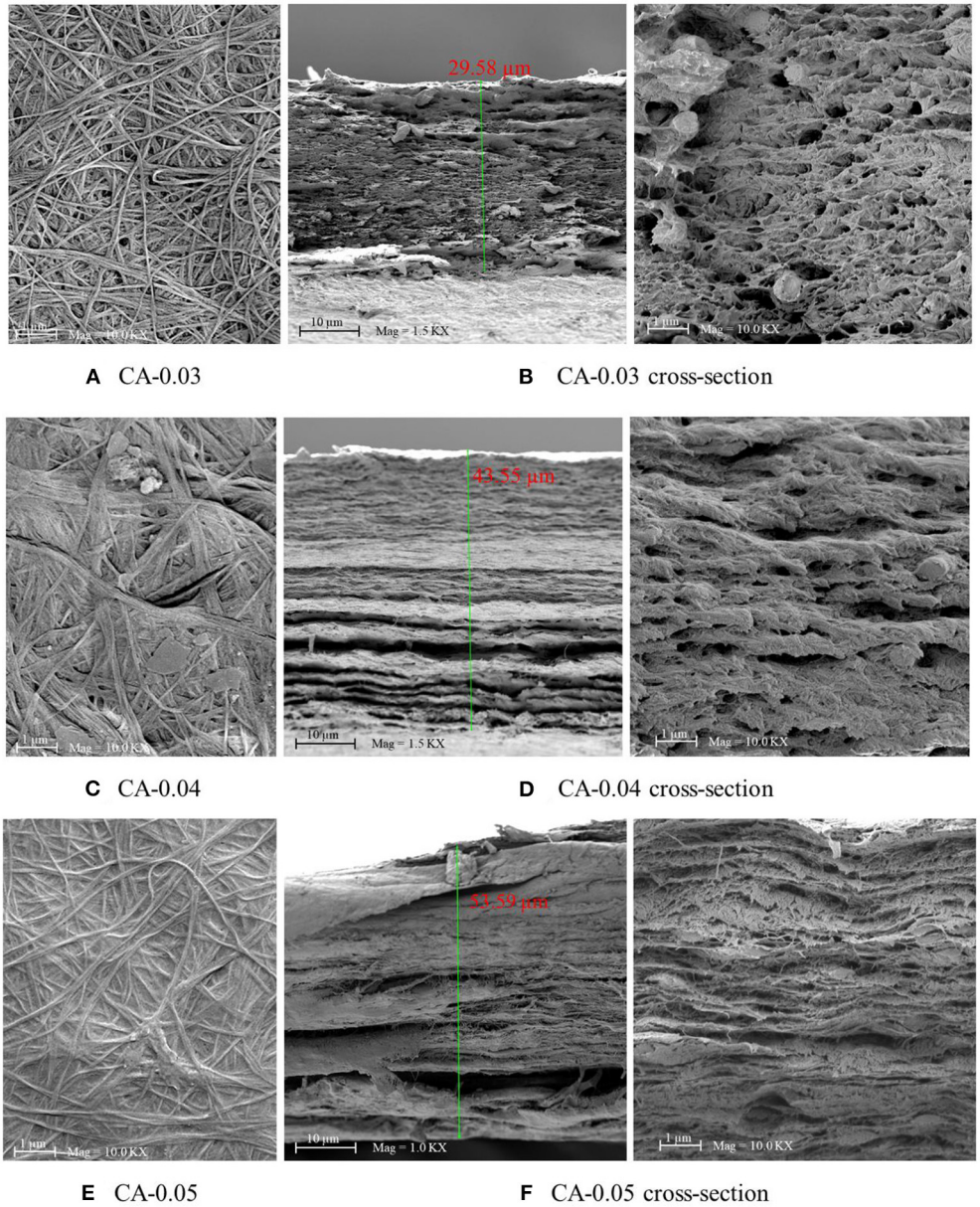

FIGURE 4 | SEM results of the CA membrane samples with various average thickness values of **(A)** CA-0.03, **(B)** CA-0.03 (cross-section), **(C)** CA-0.04, **(D)** CA-004 (cross-section), **(E)** CA-0.05, and **(F)** CA-005 (cross-section) at 10,000× magnifications, 5 kV.

as shown in **Figure 3**. **Figure 4** shows the SEM results of the normal and cross-sectional surfaces of the bio-CA membranes with three different degrees of thickness (0.03, 0.04, and 0.05 mm). As shown in **Figures 4A,C,E**, the normal surface of the membranes generally featured a rough fibrous texture packed with dense randomly entangled cellulose fibers. Meanwhile, the cross-sectional results (**Figures 4B,D,F**) revealed a multi-stack-like structure, composing of multiple thin layers of the CA fibrous sheets overlayed and stacked up together throughout the thickness of the membranes. Variation in morphological features (e.g., density and void distribution) of the membrane was observed. This stemmed from the difference in undertaking nature in the formation of BC during the cultivation stage, resulting in the asymmetric morphology of the membrane.

The CA membrane was an organic hydrocarbon compound consisting CHO elements. **Figure 5** illustrates the energy dispersive x-ray (EDX) results of the CA membranes. The element analysis revealed that the samples consisted mainly of carbon (C) and oxygen (O) with good dispersion of the components throughout the membranes. **Table 1** summarizes the carbon (C) and oxygen (O) compositions of the prepared samples.

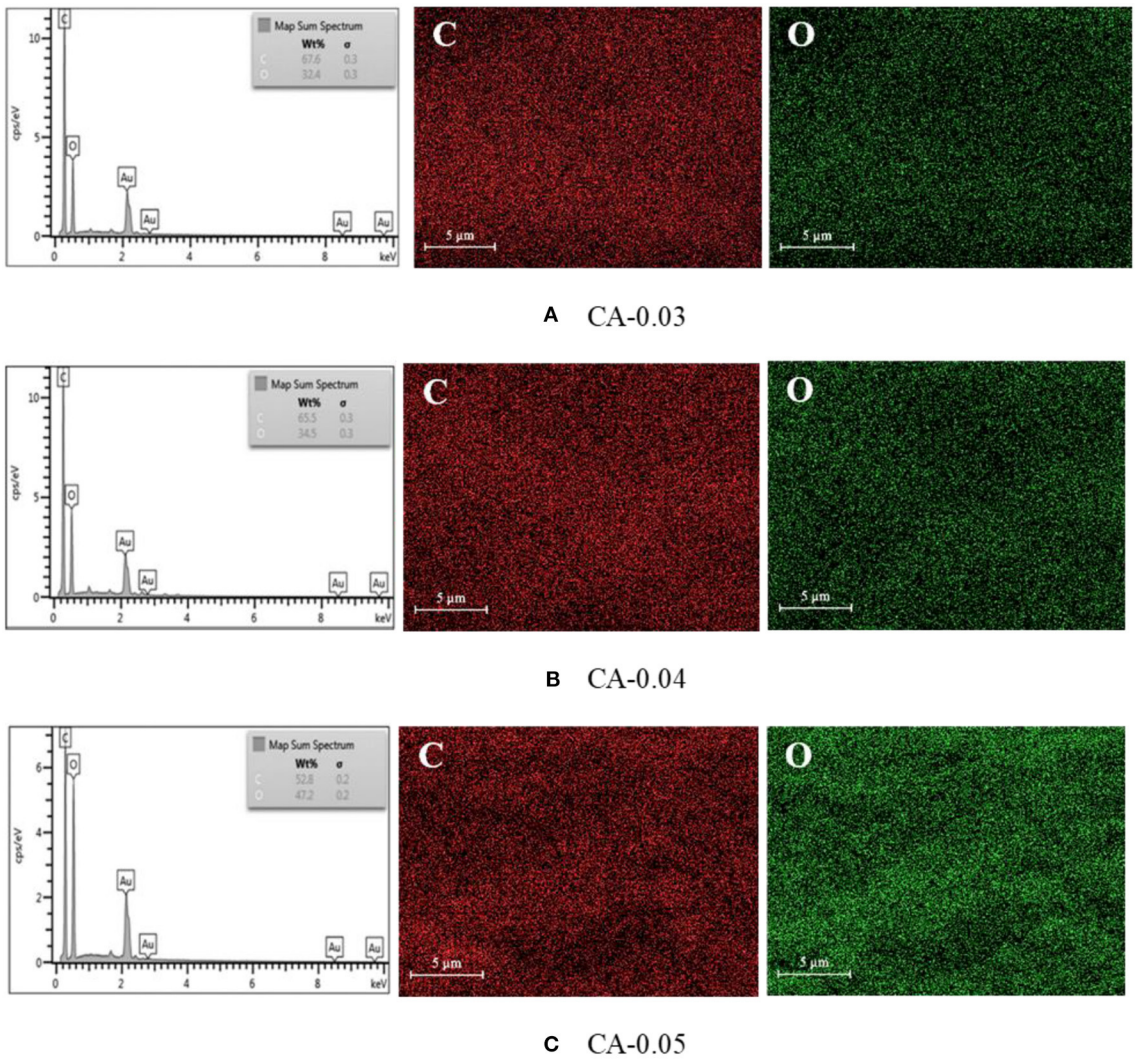

FIGURE 5 | EDX carbon (C) and oxygen (O) elemental mapping results of the CA membrane samples with various values of average thickness **(A)** CA-0.03 (thickness = 0.03 mm), **(B)** CA-0.04 (thickness = 0.04 mm), and **(C)** CA-0.05 (thickness = 0.05 mm) at 10,000× magnifications, 5 Kv.

TABLE 1 | Element composition (% wt) of the CA membranes.

Sample	Average thickness (mm)	Element composition (% wt)	
		C	O
CA-0.03	0.03	67.6	32.4
CA-0.04	0.04	65.5	34.5
CA-0.05	0.05	52.8	47.2

Chemical Structure Analysis by FTIR

The chemical structure of the prepared membranes composed mainly of the CA was revealed in the FTIR results, as shown in **Figure 6**. The FTIR spectra of the sample showed peaks corresponding to the common functional groups similar to those of the CA. The presence of the peak associated with the C=O stretching of the hemicellulose at the wavelength of 1,543 cm^{-1} was observed, altogether with the O–H stretching peak at 3,341 cm^{-1} the C–O–C vibration at 1,160 cm^{-1}, and the C<H2 vibration at 1,427 cm^{-1} of the cellulose structure, and the C=C stretching in the aromatic structure at 1,543 cm^{-1} The FTIR result was in good agreement with the characteristic peaks observed in a study by Khami et al. (2019), in which the CA material was synthesized by acetylation of BC. The magnitude of transmittance in the related spectra could be different depending on the degree of substitution of the acetyl group on the cellulose main chains.

Thermal and Mechanical Properties of the CA Membrane

Figure 7 shows the TGA result of the CA membrane. The decomposition temperature of the material was found to be

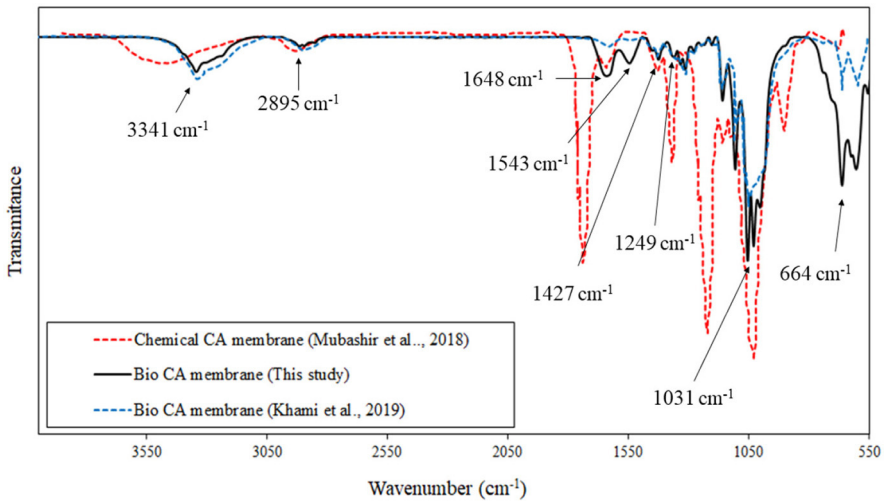

FIGURE 6 | Fourier transform infrared analysis of the CA membranes.

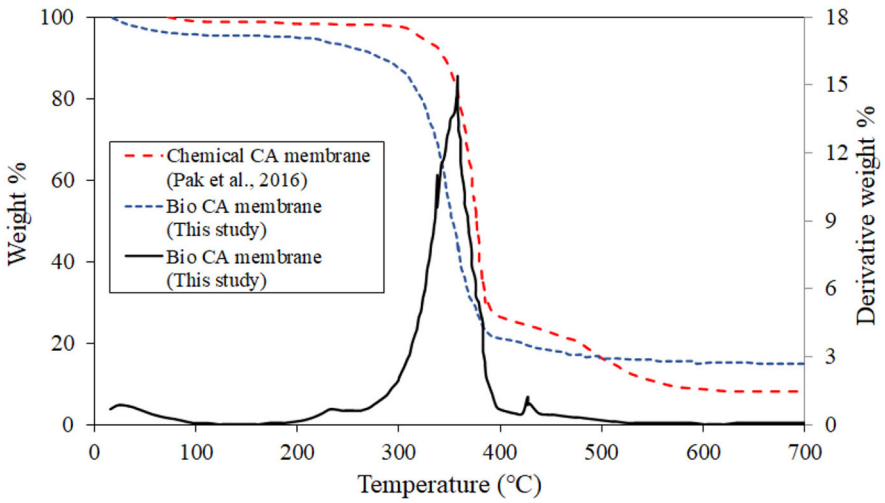

FIGURE 7 | The result of thermogravimetry analysis of the CA membrane at a heating rate of 10°C/min under a N_2 atmosphere.

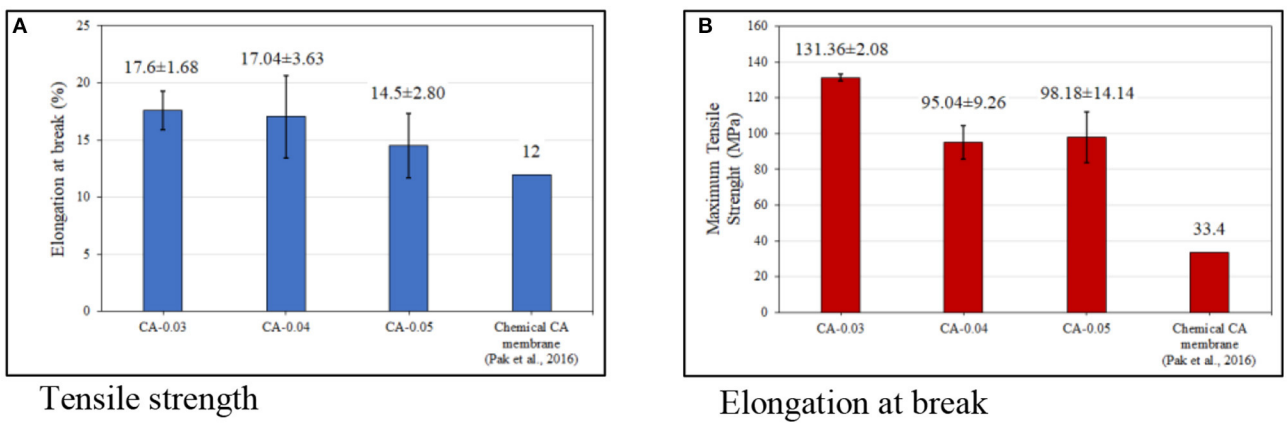

FIGURE 8 | Tensile properties of the CA membranes: **(A)** Tensile strength and **(B)** Elongation at break.

around 350°C. From room temperature to about 300°C, the TGA curve was slightly declined and almost in the plateau region, suggesting that the membrane was relatively thermally stable. This suggests the applicable range of the service temperature of the gas separation using the prepared membrane. The prepared membrane possessed similar thermal stability characteristics when compared with the CA membrane synthesized by the chemical route.

Tensile Strength of the CA Membrane

Figure 8 shows the tensile properties of the membrane samples. The average tensile strength of the membranes was in the range of 95–131 MPa. At room temperature, the membranes exhibited semi-ductile-like material characteristics under tensile. At a strain rate of 5 mm/min, the average elongation at break of the samples was ∼15–17%. For the CA-0.03 membrane (0.03 mm thick), the sample showed the highest stress value of about 131 MPa. Under tensile force, the induced orientation of the CA fibers could undergo to some extent, which seemed to be more pronounced in the thicker samples (i.e., 0.04 and 0.05 mm). With a larger thickness, the laminated thin layers of the fibrous CA probably slipped from each other under shear stress, resulting in decreased strength of the sample. Without reinforcement, the tensile strength of the pristine flat-sheet membranes prepared by the proposed bioprocess in this study is relatively higher, when compared with the neat

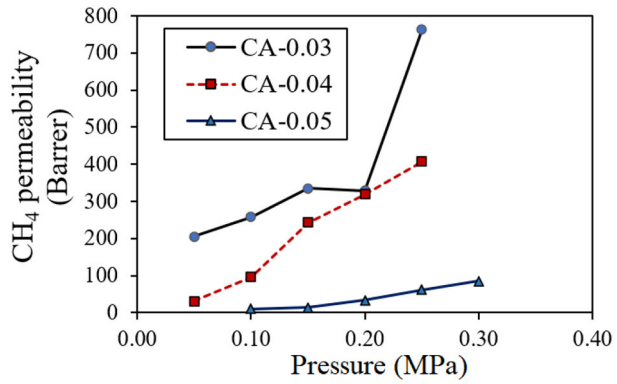

FIGURE 10 | Effect of feed pressure on CH_4 permeability (Barrer) of the permeate transported through the CA membrane with thickness values of 0.03 mm (CA-0.03), 0.04 mm (CA-0.04), and 0.05 mm (CA-0.05) at room temperature (30°C).

TABLE 2 | Gas permeation results.

Pressure (MPa)	CO_2 permeability (Barrer)[a]			CH_4 permeability (Barrer)[a]			Selectivity (CO_2/CH_4)		
	CA-0.03	CA-0.04	CA-0.05	CA-0.03	CA-0.04	CA-0.05	CA-0.03	CA-0.04	CA-0.05
0.05	374.71	456.76	-[b]	205.52	30.82	-[b]	1.82	14.82	-[b]
0.10	243.11	426.76	294.32	257.56	95.91	9.97	0.94	4.45	29.53
0.15	228.28	206.30	88.72	335.51	243.51	13.61	0.68	0.85	6.52
0.20	219.41	187.62	28.82	328.53	318.76	33.34	0.67	0.59	0.86
0.25	418.72	281.39	38.45	762.98	406.87	61.41	0.55	0.69	0.63
0.30	-[c]	-[c]	40.1	-[c]	-[c]	84.55	-[c]	-[c]	0.47

[a] *Barrer* $[10^{-10} cm^3_{(STP)}\ cm\ cm^{-2}\ s^{-1}\ cmHg^{-1}]$.

[b] *No permeate detected.*

[c] *Leak detected since the membrane was torn.*

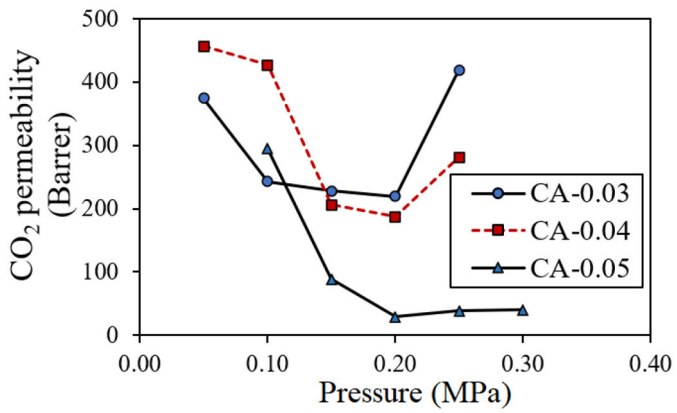

FIGURE 9 | Effect of feed pressure on CO_2 permeability (Barrer) of the permeate transported through the CA membrane with thickness values of 0.03 mm (CA-0.03), 0.04 mm (CA-0.04), and 0.05 mm (CA-0.05) at room temperature (30°C).

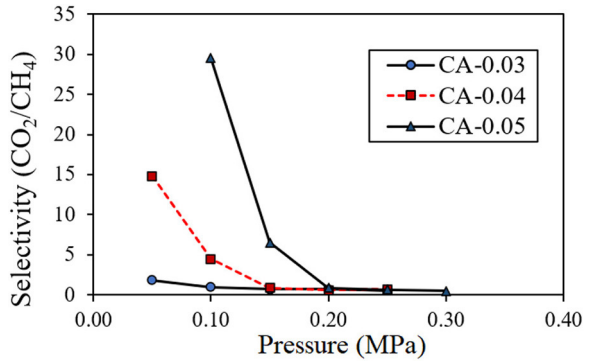

FIGURE 11 | Effect of feed pressure on the CO_2/CH_4 selectivity of permeability (Barrer) of the permeate transported through the CA membrane with thickness values of 0.03 mm (CA-0.03), 0.04 mm (CA-0.04), and 0.05 mm (CA-0.05) at room temperature (30°C).

membranes synthesized *via* the solvent casting of the CA solution (Pak et al., 2016).

CO_2 Separation Performance of the Membrane From a Binary CO_2/CH_4 Mixed Gas

The CO_2 removal capacity of the CA membranes with three degrees of thickness of 0.03 mm (CA-0.03), 0.04 mm (CA-0.04), and 0.05 mm (CA-0.05) was tested in the gas separation unit, as described earlier. The binary mixed gas containing a fixed CO_2/CH_4 ratio (40%v CO_2) was fed into the membrane unit having the CA membrane as the separating barrier at a feed pressure ranging from 0.05 to 0.3 MPa. The CH_4 and CO_2 compositions of the permeate and the retentate were obtained from GC results. The transport of the gas components in terms of permeability and selectivity were calculated from the gas

TABLE 3 | CO_2/CH_4 selectivity comparison of various CA membranes for CO_2/CH_4 system.

CA membrane	Solvent/ Modifying agent	Gas feed (CH_4/CO_2)	Feed pressure (MPa)	Thickness (mm)	CO_2 permeability (Barrer)	Selectivity (CO_2/CH_4)	References
Flat sheet*	–/–	60:40	0.1	0.05	294.32	29.53	This work
Flat sheet**	NMP/–	Pure CH_4 /Pure CO_2	0.3	N/A	34.8	10.71	Mubashir et al., 2018a
Flat sheet**	NMP/–	Pure CH_4 /Pure CO_2	0.5	N/A	449	21.48	Jami'An et al., 2016
Flat sheet**	NMP/NH_2-MIL-53(Al)	50:50	0.2	N/A	34.8	18.4	Mubashir et al., 2018b
Flat sheet**	THF/PEG	Pure CH_4 /Pure CO_2	0.2	0.03–0.04	32.58	53.98	Moghadassi et al., 2014
Hollow fiber**	NMP/PDMS	50:50	0.3	-	12,300	10.60	Mubashir et al., 2019
Hollow fiber**	THF, EtOH/ PDMS	60:40	0.7	-	129,000	43.8	Pak et al., 2016

*Bio-CA membrane.
**Chemical-CA membrane.

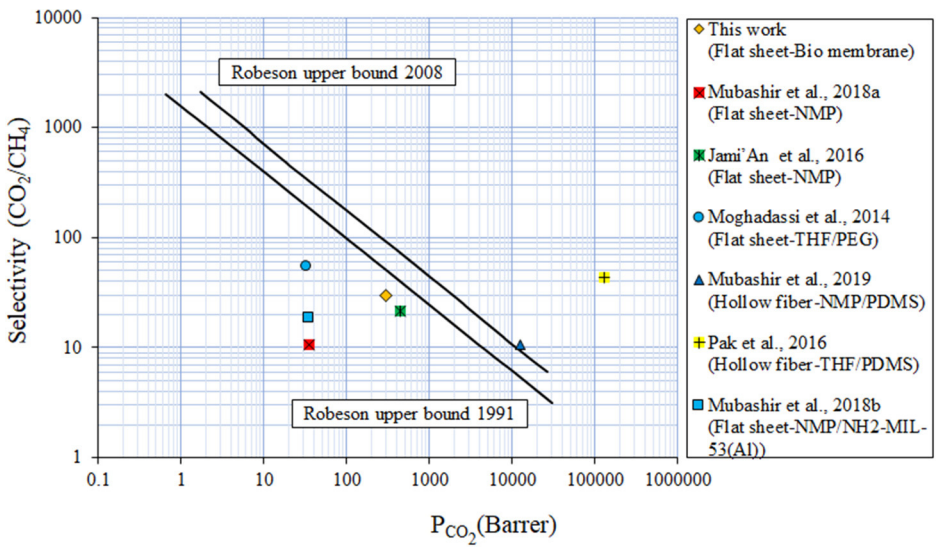

FIGURE 12 | CO_2/CH_4 gas separation performance of various CA membranes in comparison to the Robeson upper bound.

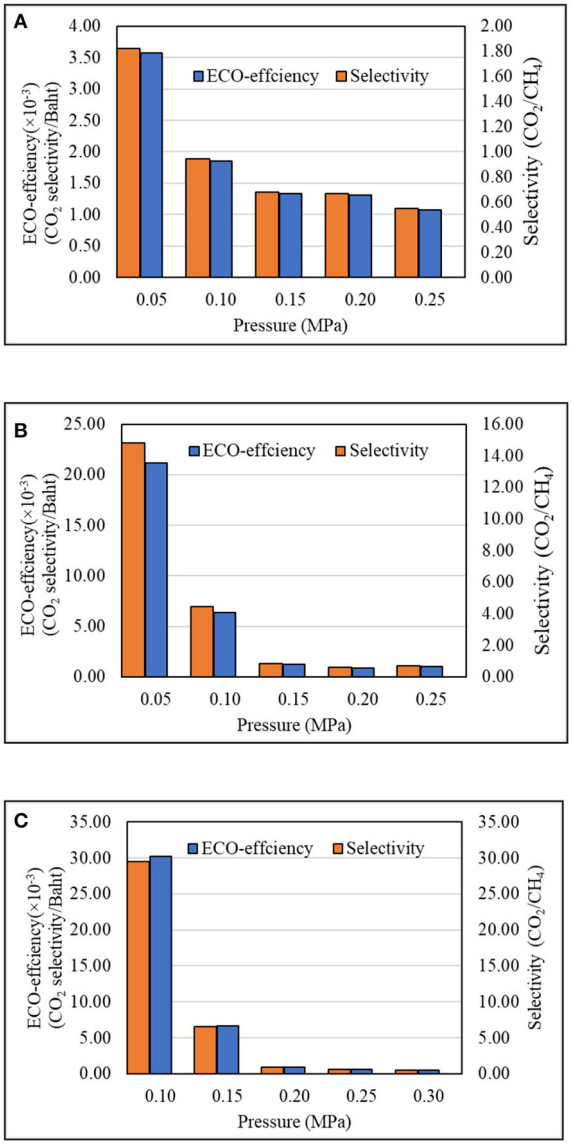

FIGURE 13 | Modified eco-efficiency of CO_2/CH_4 selectivity of the gas separation unit with the CA membranes: **(A)** CA-0.03; **(B)** CA-0.04; and **(C)** CA-0.05.

concentrations. The gas permeation results are summarized in **Table 2**.

For the binary gas mixture, both CO_2 and CH_4 competitively permeated under the pressure difference across the thickness of the asymmetric bio-CA membrane. **Figure 9** shows the effect of feed pressure on CO_2 permeability of the gas permeate passing through the membranes with various thickness values (0.03, 0.04, and 0.05 mm). With the increasing pressure of the feed, the CO_2 permeability decreased until the pressure reached around 0.2 MPa at which the curve began to climb up. **Figure 10** illustrates the effect of feed pressure on the CH_4 permeability of the gas permeate passing through the membranes with various thickness values (0.03, 0.04, and 0.05 mm). The CH_4 permeability tended to increase with the increasing feed pressure, particularly in a high-pressure region. The transport of both CO_2 and CH_4 through the dense solid CA membranes could be explained by the solution-diffusion mechanism, in which CO_2 has better solubility within the matrix relative compared to CH_4 (Ismail and Lorna, 2002). CO_2 has a greater affinity toward the CA matrix due to the polar–polar interaction between the CO_2 molecules and the acetyl/hydroxyl groups on the CA backbones. Whereas, CH_4 essentially exhibits no chemical association within the CA membrane due to its non-polar nature, and therefore, it can only be purely transported by the physical mechanism, which is limited by its low solubility on the highly polar sites in the membranes. With the incremental feed pressure, increasing the partial pressure of the CO_2 would result in higher CO_2 concentration within the CA matrix. As demonstrated in **Figure 9**, however, the CO_2 permeability decreased when the feed pressure increased from 0.05 to about 0.2 MPa. This could be explained by the membrane by the carrier saturation of the active sites within the CA membrane when all available carboxyl/hydroxyl pendant groups were associated with the chemical interactions with highly polar CO_2 molecules. (Zou and Winston Ho, 2006). Therefore, increasing the CO_2 partial pressure would not further increase the CO_2 flux since all the carriers have already reacted with CO_2 and attained the maximum capacities. As a result, the CO_2 permeability would drop. On the other hand, the transporting CH_4 did not have any chemical association with carriers. Thus, its sorption behavior could be explained by Henry's law in which the CH_4 flux linearly increased with the feed pressure, as shown in **Figure 10**.

The CO_2/CH_4 separation performance of the membrane was measured in terms of the CO_2 selectivity of the gas permeate. **Figure 11** depicts the effect of operating feed pressure on the CO_2 selectivity (CO_2/CH_4 permeability ratio) of the CA membranes having different thicknesses of 0.03, 0.04, and 0.05 mm. The CO_2 selectivity drastically declined to approach very low values as the feed pressure increased. This phenomenon could be due to the plasticization effects induced by a high concentration of the sorbed CO_2 within the asymmetric CA membrane (Houde et al., 1996; Cerveira et al., 2018). The high solubility of CO_2 may potentially swell the CA polymer to such an extent that the intermolecular interactions were disrupted, which led to the enlargement of the free volume captivities (Puleo et al., 1989; Chang et al., 2019). Consequently, the transport rate of the penetrant CO_2 and CH_4 were enhanced. From SEM results, the membrane typically inherited a multi-layered flat-sheet structure with a little degree of presented voids within the matrix. These void characteristics could also affect the transport properties, such as the surface sorption–desorption behaviors, of the permeances transporting through the membrane. As discussed earlier, the structure of the obtained thick membranes generally featured well-packed layers with less presence of interlayer voids. In a low-pressure region where the plasticization had not yet been taken, high CO_2 selectivity was achieved when using a thick membrane (i.e., CA-0.05), which exhibited a well-packed structure with fewer interlayer voids. From the graph, the plasticization pressure of the CA membranes for the separation of the CO_2/CH_4 gas mixture was observed to occur

at 0.1 MPa for CA-0.03, 0.15 MPa for CA-0.04, and 0.2 MPa for CA-0.05, respectively. A maximum CO_2/CH_4 selectivity value of 29.53 was achieved in the separation system containing the CA-0.05 membrane operating at a feed pressure of 0.10 MPa. The CO_2 selectivity of this study was in good agreement when compared with other related studies. **Table 3** summarizes the CO_2/CH_4 selectivity results in comparison with related studies on various CA membranes for CO_2/CH_4 systems. The CO_2 selectivity value of the bio-CA membrane was also plotted among the CO_2/CH_4 selectivity results obtained from the related studies in comparison to the Robeson upper bound relationship (Robeson, 2008), as shown in **Figure 12**. From the graph, the best result of the CO_2/CH_4 selectivity value of 29.53 locates under, but relatively close to, the Robeson upper bounds compared with the reported results obtained from other studies utilizing flat CA membrane systems (see **Table 3**). As discussed earlier, the flat-sheet bio-CA membranes prepared from environmental-friendly procedures proposed in this study have shown promising CO_2 removal capability for biogas treatment applications. However, an improvement on the membrane properties could be further explored to enhance its separation performance in the direction of surpassing the upper bound curve toward the commercially desirable region.

Eco-Efficiency Analysis

The total production cost of bio-CA membrane made from CJR in this study was roughly calculated as follows: The total production cost of 40 bio-CA membranes with a total area of 8,039 cm^2 was 357.62 Baht. Thus, the lab-scale production cost of bio-CA membrane from CJR in this study was ∼0.044 Baht/cm^2. However, the cost of these in-house membranes was still relatively high, compared with the commercial CA membranes which have an estimated price in the range of 0.001–0.008 Baht/cm^2 (Alibaba.com, 2021). The operating cost of the membrane separation testing in this study, estimated from the gas mixture used in each experiment, was 5.10 Baht/L. The eco-efficiencies of the CO_2 separation for three different degrees of thickness of bio-CA membranes, as calculated by Equation (6), are displayed in **Figure 13**. The results indicate that the eco-efficiency was drastically dependent on the pressure of the gas mixture fed into the separation unit. Moreover, the thickness of the CA membrane affected the eco-efficiency as well, in which the thicker the CA membrane, the higher the eco-efficiency. The cost for preparing the CA membranes with various thicknesses is not significantly different. While the thicker membranes could deliver higher CO_2 separation performance than the thinner ones, the thicker membranes are more economically attractive for potential CO_2 removal applications. it can be concluded from the results that the bio-CA-0.05 membrane was the most appropriate one to be applied in the membrane separation unit at the air inlet pressure of 0.05 MPa.

CONCLUSIONS

An eco-friendly approach to synthesize the bio-CA membrane from the cultivation of coconut water residues, potentially used for the removal of CO_2 from biogas, was successfully developed. The membranes exhibited the ability to selectively separate CO_2 from the binary CO_2/CH_4 mixed gas. The CO_2 removal capability of the bio-CA membranes in terms of the selectivity was relatively good for the neat or pristine CA membranes in which the highest CO_2 selectivity value of 29.53 was achieved. The performance to cost ratio of the CO_2 separation was evaluated in terms of the eco-efficiency of the process. The modified eco-efficiency analysis suggested that the CO_2 gas separation process using thick membranes operating at low-pressure conditions would yield higher eco-efficiency values. Using CJR as a carbon source for bio-CA membrane not only adds value to waste but also reduces environmental pollution. This study is also one of the initiatives taken in an effort to enhance the quality of biogas suitable for a wider range of applications, particularly in southern Thailand where local biogas production facilities are drastically increasing in the last few years.

DATA AVAILABILITY STATEMENT

The raw data supporting the conclusions of this article will be made available by the authors, without undue reservation.

AUTHOR CONTRIBUTIONS

AK and WD were leading researchers of the project, conceived the presented idea, supervised the findings and analysis, and prepared manuscript. SW performed the laboratory experiments and assisted in the image preparation of the manuscript. All authors contributed to the article and approved the submitted version.

ACKNOWLEDGMENTS

We would like to acknowledge the financial support from Walailak University through the WU62204 research grant.

REFERENCES

Adebayo, A., Jekayinfa, S., and Linke, B. (2015). Effects of organic loading rate on biogas yield in a continuously stirred tank reactor experiment at mesophilic temperature. *Curr. J. Appl. Sci. Technol.* 11, 1–9. doi: 10.9734/BJAST/2015/18040

Alibaba.com (2021, April 7). *Perfect Cellulose Acetate Membrane for Pure Quality Water*. Retrieved from: https://www.alibaba.com/showroom/cellulose-acetate-membrane.htmL

Barud, H. S., Araújo Júnior, A. M., Santos, D. B., Assunção, R. M. N., Meireles, C. S., Cerqueira, D. A., et al. (2008). Thermal behavior of cellulose acetate produced from homogeneous acetylation of bacterial cellulose. *Thermochimica Acta* 47, 61–69. doi: 10.1016/j.tca.2008.02.009

Basu, S., Khan, A. L., Cano-Odena, A., Liu, C., and Vankelecom, I. F. J. (2010). Membrane-based technologies for biogas separations. *Chemical Society Reviews*. 39, 750–768. doi: 10.1039/b817050a

Buchanan, C. M., Gardner, R. M., and Komarek, R. J. (1993). Aerobic biodegradation of cellulose acetate. *J Appl Polym Sci*. 47, 1709–1746. doi: 10.1002/app.1993.070471001

Cerveira, G. S., Borges, C. P., and de Kronemberger, F. A. (2018). Gas permeation applied to biogas upgrading using cellulose acetate and polydimethylsiloxane membranes. *J. Cleaner Product*. 187, 830–838. doi: 10.1016/j.jclepro.2018.03.008

Chang, M., Deng, L., Xiang, D., Cao, B., Hosseini, S. S., and Li, P. (2019). Approaches to suppress CO2-induced plasticization of polyimide membranes in gas separation applications. *Processes*. 7:51. doi: 10.3390/pr7010051

Changwichan, K., Silalertruksa, T., and Gheewala, S. (2018). Eco-efficiency assessment of bioplastics production systems and end-of-life options. *Sustainability*. 10:952. doi: 10.3390/su10040952

Chen, X., Vinh, H., Avalos Ramirez, A., Rodrigue, D., and Kaliaguine, S. (2015). Membrane gas separation technologies for biogas upgrading. *RSC Adv*. 5:666. doi: 10.1039/C5RA00666J

Elfiana, T. N., Fitria, A. N. I., Sedyadi, E., Prabawati, S. Y., and Nugraha, I. (2018). Degradation study of biodegradable plastic using nata de coco as a filler. *Biol. Med. Natur. Product Chem*. 7, 33–38. doi: 10.14421/biomedich.2018.72.33-38

Gardner, R. M., Buchanan, C. M., D., Dorschel, R. K., Boggs, C., and White, A. W. (1994). Compostability of cellulose acetate films. *J. Appl. Polym. Sci*. 52, 1477–1488. doi: 10.1002/app.1994.070521012

Gu, J.-D., Eberiel, D. T., McCarthy, S. P., and Gross, R. A. (1993). Cellulose acetate biodegradability upon exposure to simulated aerobic composting and anaerobic bioreactor environments. *J. Environ. Polym Degr*. 1, 143–153. doi: 10.1007%252FBF01418207

Heilala, J., Ruusu, R., Montonen, J., Vatanen, S., Kavka, C., Asnicar, F., et al. (2014). "Eco-process engineering system for collaborative product process system optimisation," in *Advances in Production Management Systems. Innovative and Knowledge-Based Production Management in a Global-Local World*, Vol 439, eds B. Grabot, B. Vallespir, S. Gomes, A. Bouras, & D. Kiritsis (Berlin, Heidelberg: Springer Berlin Heidelberg), 634–641. doi: 10.1007/978-3-662-44736-9_77

Houde, A., Krishnakumar, B., Charati, S., and Stern, S. (1996). Permeability of dense (homogeneous) cellulose acetate membranes to methane, carbon dioxide, and their mixtures at elevated pressures. *J. Appl. Polym. Sci*. 62, 2181–2192. doi: 10.1002/(SICI)1097-4628(19961226)62:13<2181::AID-APP1>3.0.CO;2-F

Ismail, A. F., and Lorna, W. (2002). Penetrant-induced plasticization phenomenon in glassy polymers for gas separation membrane. *Separat. Purif. Techn*. 27, 173–194. doi: 10.1016/S1383-5866(01)00211-8

Jami'An, W. N. R., Hasbullah, H., Mohamed, F., Yusof, N., Ibrahim, N., and Ali, R. R. (2016). Effect of evaporation time on cellulose acetate membrane for gas separation. *IOP Confer. Series Earth Environ. Sci*. 36:8. doi: 10.1088/1755-1315/36/1/012008

Khami, S., Khamwichit, W., and Suwannahong, K. (2019). Synthesis of cellulose acetate nanofiber (CANF) from bacterial cellulose (BC) incubated from cannery seafood wastewater (CSW) using acetobacter xylinum. *ARPN J. Eng. Appl. Sci*. 14, 3038–3045. Retrieved from: http://www.arpnjournals.org/jeas/research_papers/rp_2019/jeas_0919_7904.pdf

Khami, S., Khamwichit, W., Suwannahong, K., and Sanongraj, W. (2014). Characteristics of bacterial cellulose production from agricultural wastes. *Adv. Mater. Res*. 931–932, 693–697. doi: 10.4028/www.scientific.net/AMR.931-932.693

Komarek, R. J., Gardner, R. M., Buchanan, C. M., and Gedon, S. (1993). Biodegradation of radiolabeled cellulose acetate and cellulose propionate. *J. Appl. Polym Sci*. 50, 1739–1746. doi: 10.1002/app.1993.070501009

Kongruang, S. (2008). Bacterial Cellulose Production by *Acetobacter xylinum* Strains from Agricultural Waste Products. *Appl Biochem Biotechnol*,148, 245–256. doi: 10.1007/s12010-007-8119-6

Lestari, P., Elfrida, N., Suryani, A., and Suryadi, Y. (2014). Study on the production of bacterial cellulose from *Acetobacter xylinum* using agro-waste. *Jordan J. Biol. Sci*. 7, 75–80. doi: 10.12816/0008218

Liu, H., Yang, R., Zhou, Z., and Huang, D. (2020). Regional green eco-efficiency in china: considering energy saving, pollution treatment, and external environmental heterogeneity. *Sustainability (Switzerland)* 12:7059. doi: 10.3390/su12177059

Moghadassi, A. R., Rajabi, Z., Hosseini, S. M., and Mohammadi, M. (2014). Fabrication and modification of cellulose acetate-based mixed matrix membrane: gas separation and physical properties. *J. Industr. Eng. Chem*. 20, 1050–1060. doi: 10.1016/j.jiec.2013.06.042

Mubashir, M., Fong, Y. Y., Leng, C. T., and Keong, L. K. (2018a). Enhanced gases separation of cellulose acetate membrane using n-methyl-1-2 pyrrolidone as fabrication solvent. *Int. J. Autom. Mech. Eng*. 15, 4978–4986. doi: 10.15282/ijame.15.1.2018.7.0386

Mubashir, M., Fong, Y. Y., Leng, C. T., Keong, L. K., and Jusoh, N. (2020). Study on the effect of process parameters on CO_2/CH_4 binary gas separation performance over NH_2-MIL-53(Al)/cellulose acetate hollow fiber mixed matrix membrane. *Polymer Testing* 81:106223. doi: 10.1016/j.polymertesting.2019.106223

Mubashir, M., Yeong, Y. F., Lau, K. K., and Chew, T. L. (2019). Effect of spinning conditions on the fabrication of cellulose acetate hollow fiber membrane for CO_2 separation from N_2 and CH_4. *Polymer Testing*. 73, 1–11. doi: 10.1016/j.polymertesting.2018.10.036

Mubashir, M., Yeong, Y. F., Lau, K. K., Chew, T. L., and Norwahyu, J. (2018b). Efficient CO_2/N_2 and CO_2/CH_4 separation using NH_2-MIL-53(Al)/cellulose acetate (CA) mixed matrix membranes. *Separat. Purif. Techn*. 199, 140–151. doi: 10.1016/j.seppur.2018.01.038

Pa'e, N., Zahan, K. A., and Muhamad, I. I. (2011). Production of biopolymer from Acetobacter xylinum using different fermentation methods. *Int. J. Eng. Technol*. 11, 74–79. Retrieved from: http://ijens.org/Vol_11_I_05/116901-05-3434-IJET-IJENS.pdf

Pak, S. H., Jeon, Y. W., Shin, M. S., and Koh, H. C. (2016). Preparation of cellulose acetate hollow-fiber membranes for CO_2/CH_4 Separation. *Environ. Eng. Sci*. 33, 17–24. doi: 10.1089/ees.2015.0201

Phruksaphithak, N., Kaewnun, C., and and, O.-,Thong, S. (2019). Bacterial cellulose production and applications. *Sci. Eng. Health Studies* 13, 1–7. doi: 10.14456/sehs.2019.1

Puleo, A. C., Paul, D. R., and Kelley, S. S. (1989). The effect of degree of acetylation on gas sorption and transport behavior in cellulose acetate. *J. Membr. Sci*. 47, 301–332. doi: 10.1016/S0376-7388(00)83083-5

Rivard, C. J., Adney, W. S., Himmel, M. E., Mitchell, D. J., Vinzant, T. B., Grohmann, K., et al. (1992). Effects of natural polymer acetylation on the anaerobic bioconversion to methane and carbon dioxide. *Appl. Biochem. Biotechnol*. 34–35, 725–736. doi: 10.1007/BF02920592

Robeson, L. M. (2008). The upper bound revisited. *J. Membr. Sci*. 320, 390–400. doi: 10.1016/j.memsci.2008.04.030

Sanaeepur, H., Ahmadi, R., Sinaei, M., and Kargari, A. (2019). Pebax-modified cellulose acetate membrane for CO_2/N_2 separation. *J. Membr. Sci. Res*. 5, 25–32. doi: 10.22079/JMSR.2018.85813.1190

Tafreshi, N., Sharifnia, S., and Moradi Dehaghi, S. (2017). Box–Behnken experimental design for optimization of ammonia photocatalytic degradation by ZnO/Oak charcoal composite. *Process Safet. Environ. Protect*. 106, 203–210. doi: 10.1016/j.psep.2017.01.015

Zou, J., and Winston Ho, W. S. (2006). CO_2-selective polymeric membranes containing amines in crosslinked poly(vinyl alcohol). *J. Membr. Sci*. 286, 310–321. doi: 10.1016/j.memsci.2006.10.013

Conflict of Interest: The authors declare that the research was conducted in the absence of any commercial or financial relationships that could be construed as a potential conflict of interest.